

Gas-Phase Structures of Acetyl Peroxynitrate and Trifluoroacetyl Peroxynitrate

Angelika Hermann,[†] Jan Niemeyer,[†] Hans-Georg Mack,[†] Radion Kopitzky,[‡]
 Michaela Beuleke,[‡] Helge Willner,[‡] Dines Christen,[†] Martin Schäfer,[§] Alfred Bauder,[§] and
 Heinz Oberhammer^{*,†}

Institut für Physikalische und Theoretische Chemie, Universität Tübingen, D-72076 Tübingen, Germany, Anorganische Chemie, Gerhard-Mercator-Universität Duisburg, D-47048 Duisburg, Germany, and Laboratorium für Physikalische Chemie, Eidgenössische Technische Hochschule, Zürich, CH-8092 Zürich, Switzerland

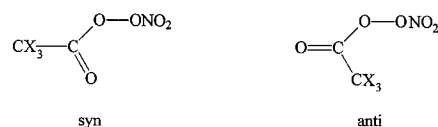
Received September 22, 2000

The molecular structures and conformational properties of acetyl peroxynitrate (PAN, CH₃C(O)OONO₂) and trifluoroacetyl peroxynitrate (FPAN, CF₃C(O)OONO₂) were investigated in the gas phase by electron diffraction (GED), microwave spectroscopy (MW), and quantum chemical methods (HF/3-21G, HF/6-31G*, MP2/6-31G*, B3PW91/6-31G*, and B3PW91/6-311+G*). All experimental and theoretical methods show the syn conformer (C=O bond of acetyl group syn to O–O bond) to be strongly predominant relative to the anti conformer. The O–NO₂ bonds are extremely long, 1.492(7) Å in PAN and 1.526(10) Å in FPAN, which correlates with their low bond energy and the easy formation of CX₃C(O)OO* and *NO₂ radicals in the atmosphere. The O–O bonds (1.418(12) Å in PAN and 1.408(8) Å in FPAN) are shorter than that in hydrogen peroxide (1.464 Å). In both compounds the C–O–O–N dihedral angle is close to 85°.

Introduction

Besides ozone, acetyl peroxynitrate, CH₃C(O)OONO₂ (peroxyacetyl nitrate, PAN), is the most abundant photooxidant component in the atmosphere, especially in summer smog. It is formed in oxidative degradation of many organic compounds. It can cause eye and throat irritation and plant damages and reacts with biologically important substances, such as enzymes.¹ Extensive field measurements have shown that PAN is ubiquitous in the atmosphere and that its concentrations can exceed those of NO_x in clean tropospheric conditions.² Halogenated acetyl peroxynitrates, such as trifluoroacetyl peroxynitrate (CF₃C(O)OONO₂, FPAN), have been detected in the atmosphere only in recent years. It is formed from chlorofluorocarbon (CFC) replacements, such as HFC-143 (CH₃CF₃), which contain a CF₃C moiety that may convert into CF₃C(O)OO* radicals.^{3,4} This peroxy radical can react with NO₂ to form FPAN.^{3,5} Both peroxynitrates, PAN and FPAN, are important reservoir species for CX₃C(O)OO* radicals and provide a mechanism for NO₂ transport.² Because of the importance of these substances in atmospheric chemistry, properties such as chemical stability, UV absorption cross sections,^{6,7} IR,^{7,8} and NMR spectra⁷ have

Chart 1



been reported. The chemical stability is characterized by the low CX₃C(O)OO–NO₂ bond energies of 28(1) kcal mol⁻¹.^{3,9} In the present study we report a structure investigation of PAN and FPAN by gas electron diffraction (GED), microwave spectroscopy, and quantum chemical calculations.

PAN and FPAN can exist in two conformeric forms, with the acetyl C=O bond syn or anti with respect to the peroxide O–O bond (Chart 1). Spectroscopic investigations of PAN (IR (gas), Raman (liquid), IR (matrix), and ¹H NMR) demonstrated the presence of essentially a single conformer, with a contribution of about 1% of a second form, according to NMR data.⁷ However, for FPAN there was no indication of a second conformer.⁷ Also, in GED experiments it is difficult to detect small contributions of a second conformer. Various quantum chemical calculations (see below) predict energy differences larger than 2.7 kcal mol⁻¹ between syn and anti forms for both PAN and FPAN and thus are in agreement with the spectroscopic observations.^{7,8} To obtain additional spectroscopic data for air monitoring and unambiguous information about the conformational properties, an (unsuccessful) effort was made to record the microwave spectrum of FPAN at ambient temperatures. Subsequently, only the most stable syn conformer was detected in a supersonic jet using a pulsed nozzle Fourier transform microwave (FTMW) spectrometer.

Experiment

Caution! FPAN and especially PAN are potentially explosive.

- (8) Bruckmann, P. W.; Willner, H. *Environ. Sci. Technol.* **1983**, *17*, 352.
 (9) Bridier, I.; Caralp, F.; Loirat, H.; Lesclaux, R.; Vegret, B.; Becker, K. H.; Reimer, A.; Zabel, F. *J. Phys. Chem.* **1991**, *95*, 3594.

[†] Universität Tübingen.

[‡] Gerhard-Mercator-Universität Duisburg.

[§] Eidgenössische Technische Hochschule.

- (1) Seefeld, S.; Kinnison, D. J.; Kerr, J. A. *J. Phys. Chem. A* **1997**, *101*, 55.
 (2) Singh, B. H.; Salast, L. J.; Viezee, W. *Nature* **1986**, *321*, 588 and references therein.
 (3) Wallington, T. J.; Sehested, J.; Nielsen, O. *J. Chem. Phys. Lett.* **1994**, *226*, 563.
 (4) Maricq, M.; Szeute, J. J.; Khitrov, G. A.; Francisco, J. S. *J. Phys. Chem.* **1994**, *100*, 4514.
 (5) Zabel, F.; Kirchner, F.; Becker, K. H. *Int. J. Chem. Kinet.* **1994**, *26*, 827.
 (6) Libuda, H. G.; Zabel, F. *Ber. Bunsen-Ges. Phys. Chem.* **1995**, *99*, 1205.
 (7) Kopitzky, R.; Beuleke, M.; Balzer, G.; Willner, H. *Inorg. Chem.* **1997**, *36*, 1994.

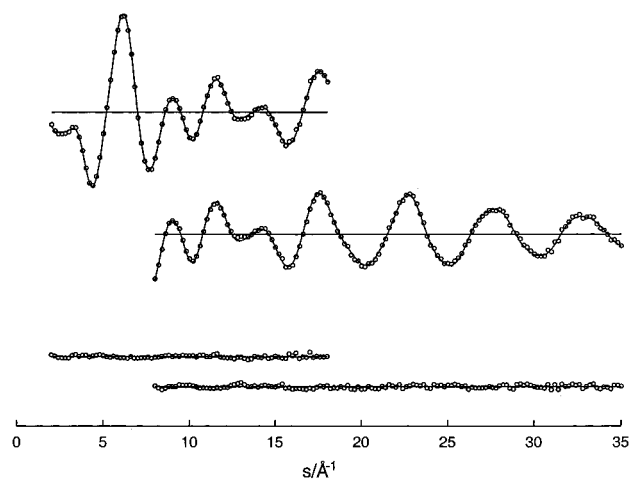


Figure 1. Experimental (dots) and calculated (full line) molecular intensities and differences for PAN.

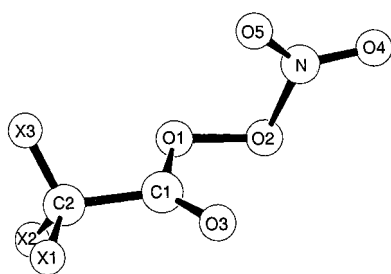


Figure 2. Molecular model for PAN (X = H) and FPAN (X = F) with atom numbering.

PAN and FPAN were synthesized and purified according to the methods described in ref 8. Electron diffraction intensities were recorded with a Gaskdiffraktograph KD-G2¹⁰ at 25 and 50 cm nozzle-to-plate distances and with an accelerating voltage of about 60 kV. The sample reservoirs were kept at +8 °C (PAN) and -33 °C (FPAN), and the inlet system and nozzle were at room temperature. The photographic plates were analyzed with the usual methods.¹¹ Averaged molecular intensities for PAN in the s ranges of 2–18 and 8–35 Å⁻¹ in steps of $\Delta s = 0.2$ Å⁻¹ are shown in Figure 1 ($s = (4\pi/\lambda) \sin \theta/2$, $\lambda =$ electron wavelength, $\theta =$ scattering angle). The intensities for FPAN are very similar and are not shown.

The observation of the microwave spectrum of CF₃C(O)OONO₂ was first attempted with a Stark spectrometer in Tübingen at ambient temperature. Only transitions due to OCF₂ and NO₂ were detected, however, and flowing the sample through the aluminum waveguide cell or using a glass cell only reduced the intensity of these decomposition products but did not show any new transitions. It was realized that the partition function even in the ground vibrational state was too unfavorable to allow a detection because of the existence of four possible internal rotations around single bonds in CF₃C(O)OONO₂.

The rotational spectrum of CF₃C(O)OONO₂ was recorded between 8 and 12 GHz with a pulsed nozzle Fourier transform microwave spectrometer in Zürich. The design of the spectrometer, which is similar to that described first by Balle and Flygare,¹² was reported previously.¹³ For the initial broadband scans, the gas mixture of approximately 1% CF₃C(O)OONO₂ in argon at a pressure of 0.8 bar was introduced via an electromechanical valve perpendicular to the Fabry-Pérot resonator.

(10) Oberhammer, H. *Molecular Structures by Diffraction Methods*; Chemical Society: London, 1976; Vol. 4, p 24.

(11) Oberhammer, H.; Gombler, W.; Willner, H. *J. Mol. Struct.* **1981**, *70*, 273.

(12) Balle, T. J.; Flygare, W. H. *Rev. Sci. Instrum.* **1981**, *52*, 33.

(13) Bettens, F. L.; Bettens, R. P. A.; Bauder, A. In *Jet Spectroscopy and Molecular Dynamics*; Hollas, J. M., Phillips, D., Eds.; Blackie Academic & Professional: Glasgow, 1995; pp 1–28.

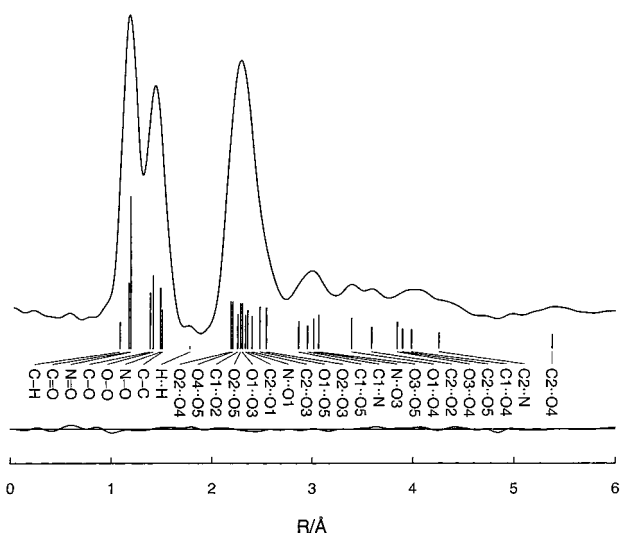


Figure 3. Experimental radial distribution function and difference curve for PAN. The positions of important interatomic distances are shown by vertical bars.

Table 1. Experimental and Calculated Geometric Parameters for CH₃C(O)OONO₂ (PAN)

	GED ^a		MP2/ 6-31G* ^f	B3PW91/ 6-311+G* ^f	HF/ 3-21G ^f
Distances (Å)					
C=O	1.184 ^b		1.205	1.188	1.183
(N=O) _{mean}	1.193(2)	p_1	1.205	1.184	1.212
C–C	1.505[10] ^c		1.499	1.496	1.495
O–C	1.395(12)	p_2	1.402	1.402	1.423
O–N	1.492(7)	p_3	1.543	1.504	1.472
O–O	1.418(12)	p_4	1.424	1.390	1.436
(C–H) _{mean}	1.090 ^b		1.091	1.091	1.081
Angles (deg)					
O–C=O	125.7(25)	p_5	123.7	123.2	122.1
O–C–C	107.7(16)	p_6	107.4	107.8	106.4
O=N=O	135.1(56)	p_7	135.1	133.8	132.0
Δ ONO ^d	7.2 ^b		7.5	7.2	6.3
O–O–C	107.3(13)	p_8	110.1	111.9	111.2
O–O–N	108.6(20)	p_9	107.4	109.8	107.4
H–C–H	109.4 ^b		109.4	109.1	109.5
ϕ (O–O–C=O) ^e	-3.0 ^b		-3.7	-2.9	-0.6
ϕ (O–O–N=O) ^e	2.0 ^b		0.4	2.0	7.4
ϕ (C–O–O–N)	84.7(13)	p_{10}	80.2	85.7	84.7

^a r_a values, uncertainties in parentheses are 3σ values and include systematic errors due to constraints (see text). ^b Not refined. ^c Assumed value with estimated uncertainty in brackets. ^d Δ ONO = \angle O–N=O5 – \angle O–N=O4. For atom numbering, see Figure 2. ^e Torsion of the CH₃C(O) and NO₂ groups around the O–C and O–N bonds, respectively. Both torsions lead to a decrease of the O3...O5 distance. ^f Mean values are given for parameters that are not unique.

Two separate microwave pulses of 1 μ s duration with a peak power of 1 mW were applied to each gas pulse. The polarization decays of the sample molecules were digitized at a rate of 10 MHz for 1024 channels. The data of 600–6000 gas pulses were added in the time domain in order to improve the signal-to-noise ratio. The conventional amplitude spectrum was obtained from the fast Fourier transform of the time domain data. Accurate peak frequencies of selected transitions were determined from the time domain data when the gas was introduced along the resonator axis through one of the mirrors. Higher resolution was achieved with this arrangement.

Structure Analyses

Radial distribution curves (RDF's) were obtained by Fourier transformation of the molecular intensities. Analysis of the RDF's demonstrated that both compounds exist in the syn

Table 5. Observed Rotational Transitions (MHz) in CF₃C(O)OONO₂

$J'_{K-K+} \leftarrow J''_{K-K+}$	$F' \leftarrow F''$	exptl frequency	exptl - calcd	
2 ₂₀	1 ₁₀	2 1	8637.387	0.008
		3 2	8637.400	-0.014
		1 0	8637.424	0.002
2 ₂₁	1 ₁₁	1 0	8638.609	-0.004
		2 1	8638.621	0.002
		3 2	8638.638	0.002
3 ₂₁	2 ₁₁	3 2	9855.648	0.004
		2 1	9855.698	0.000
		4 3	9855.698	0.020
3 ₂₂	2 ₁₂	3 2	9859.334	0.023
		4 3	9859.334	-0.010
		2 1	9859.356	0.003
4 ₂₂	3 ₁₂	4 3	11073.292	-0.006
		5 4	11073.324	-0.002
		3 2	11073.333	-0.005
4 ₂₃	3 ₁₃	3 3	11080.635	0.006
		4 3	11080.651	-0.003
		5 4	11080.668	0.006
5 ₁₄	4 ₀₄	3 2	11080.668	0.002
		4 4	11080.668	-0.013
		6 5	8172.978	-0.001
5 ₂₃	4 ₁₃	4 3	8172.974	0.001
		5 4	8172.978	0.000
		4 3	12290.365	-0.003
5 ₂₄	4 ₁₄	6 5	12290.365	0.004
		5 4	12290.340	0.002
		5 4	12302.576	-0.005
6 ₁₅	5 ₀₅	6 5	12302.576	-0.007
		4 3	12302.587	0.001
		5 4	9396.118	-0.001
7 ₁₆	6 ₀₆	7 6	9396.122	0.002
		6 5	9396.127	-0.000
		6 5	10619.875	-0.000
8 ₁₇	7 ₀₇	8 7	10619.879	0.003
		7 6	10619.885	0.000
		7 6	11844.236	-0.002
9 ₀₉	8 ₁₇	9 8	11844.241	0.002
		8 7	11844.247	-0.001
		9 8	8886.729	-0.000
10 ₀₁₀	9 ₁₈	10 9	8886.736	-0.002
		8 7	8886.741	0.000
		10 9	10100.574	0.002
		11 10	10100.579	-0.001
		9 8	10100.583	0.000

PAN. The RDF is shown in Figure 3. In addition to the assumptions described above, the C–H bond length and the H–C–H angle were set to the theoretical values. Ten geometric parameters p and seven vibrational amplitudes l (see Tables 1 and 2 for numbering) were refined simultaneously, and the following correlation coefficients had values larger than $|0.7|$: $p_2/p_4 = -0.79$, $p_5/p_7 = 0.83$, $p_7/p_9 = 0.89$, $p_4/l_2 = 0.73$, and $p_5/l_4 = -0.74$. The final results are listed together with calculated values in Table 1 (geometric parameters) and Table 2 (vibrational amplitudes).

FPAN. For the RDF see Figure 4. In addition to the assumptions described above, the O–C bond length was constrained to 1.360 Å with an estimated uncertainty of ± 0.01 Å. This value was chosen on the basis of the theoretical calculations and the experimental value for PAN. The calculations predict this bond in FPAN to be shorter by about 0.03 Å than that in PAN (see Tables 1 and 3). Furthermore, the O=N–O angle was set to a mean theoretical value. Ten geometric parameters p and six vibrational amplitudes l were refined simultaneously, and the following correlation coefficients had values larger than $|0.7|$: $p_4/p_9 = 0.74$, $p_8/p_{10} = -0.70$, $p_{10}/l_2 = -0.80$, and $l_2/l_3 = 0.83$. The final results are listed together with the calculated values in Table 3 (geometric parameters) and Table 4 (vibrational amplitudes).

Table 6. Rotational, Centrifugal Distortion, and ¹⁴N Nuclear Quadrupole Coupling Constants (MHz) and Dipole Moments (D) of CF₃C(O)OONO₂

parameter	MW spectra ^a	GED	B3PW91/6-31G*
A	2676.0918(3)	2680.9	2679.9
B	610.3603(1)	596.8	600.2
C	609.1355(1)	592.7	597.3
$\Delta_J \times 10^3$	0.0686(6)		
$\Delta_{JK} \times 10^3$	0.1694(107)		
$\Delta_K \times 10^3$	0.0009(3)		
χ_{aa}	0.151(7)		
χ_{bb}	-0.108(7)		
χ_{cc}	-0.044(7)		

^a In parentheses is σ in units of the last decimal place.

Table 7. Calculated Energy Differences $\Delta E = E(\text{anti}) - E(\text{syn})$ (kcal mol⁻¹) of the Conformers of the Investigated Peroxynitrates

method	HF/3-21G	HF/6-31G*	MP2/6-31G*	B3PW91/6-31G*	B3PW91/6-311+G*
PAN	4.8	5.2	3.9	3.2	3.5
FPAN	4.7	5.2	2.7	3.3	4.1

Assignments and Analysis of the Rotational Spectrum. The frequencies of rotational transitions of FPAN were predicted from the moments of inertia that were calculated for the GED structure. The components of the permanent electric dipole moment were expected to have appreciable values mainly in the direction of the c principal axis of the nearly prolate symmetric top. Because of the large moment of inertia of the CF₃ group and the relatively high predicted barrier (1.1 kcal mol⁻¹; see below), internal rotation splittings are neither expected nor observed in the high-resolution spectrum. The first μ_c -type R-branch transitions were readily identified near the predicted positions of the syn conformer. They showed the typical hyperfine splittings from the ¹⁴N quadrupole nucleus in FPAN. Finally, 14 transitions were assigned with angular momentum quantum numbers J between 1 and 10. The frequencies of their hyperfine components are listed in Table 5. No transitions were observed near the predicted frequencies of the anti conformer.

Rotational constants, three quartic centrifugal distortion constants and the diagonal quadrupole coupling constants were fitted to the measured transition frequencies using Pickett's program.²⁰ The results are collected in Table 6. The centrifugal distortion constants are defined in Watson's asymmetric reduction in the prolate I' representation. The asymmetry parameter κ turned out to be -0.9988 , very near the prolate limit of -1 .

It was not attempted to combine rotational constants with GED data in the determination of the geometric structure. Since FPAN possesses four torsional vibrations around single bonds (C–C, O–C, O–O, and O–N), it is expected to undergo several large-amplitude motions. In such cases the traditional methods for calculating vibrational corrections ($\Delta r = r_a - r_z$ and $\Delta B^i = B_0^i - B_z^i$), which are derived for small amplitude vibrations, cannot be applied.

Quantum Chemical Calculations

The geometries of syn and anti conformers for both peroxy-nitrates were fully optimized with ab initio (HF/3-21G, HF/6-31G*, and MP2/6-31G*) and DFT methods (B3PW91/6-31G* and B3PW91/6-311+G*) using the Gaussian 94 program suite.²¹ The calculated energy differences between syn and anti conformers are listed in Table 7. For both compounds the syn form

Table 8. Experimental Skeletal Geometric Parameters of Peroxides with Electron-Withdrawing Substituents

	O—O (Å)	O—C (Å)	O—N (Å)	O—O—C (deg)	O—O—N (deg)	$\phi(\text{COOX})$ (deg)
CF ₃ OOCF ₃ ^a	1.419(20)	1.399(9)		107.2(12)		123.3(40)
FC(O)OOC(O)F ^b	1.419(9)	1.355(4)		109.4(9)		83.5(14)
FC(O)OONO ₂ ^c	1.420(6)	1.355[10] ^e	1.514(6)	107.5(10)	106.7(12)	86.2(14)
CF ₃ OONO ₂ ^d	1.414(8)	1.378[12] ^e	1.523(7)	107.7(14)	108.4(13)	105.1(16)
CH ₃ C(O)OONO ₂	1.418(12)	1.395(12)	1.492(7)	107.3(13)	108.6(20)	84.7(13)
CF ₃ C(O)OONO ₂	1.408(8)	1.360[10] ^e	1.526(10)	107.6(20)	109.9(15)	85.8(29)

^a Reference 25. ^b Reference 26. ^c Reference 27. ^d Reference 28. ^e Not refined in GED analysis. Estimated uncertainty is in brackets.

is predicted to be strongly favored. The CH₃ and CF₃ groups adopt eclipsed orientations with respect to the carbonyl C=O bond. The barrier to internal rotation of the CF₃ group in FPAN is predicted to be 1.1 kcal mol⁻¹ (B3PW91/6-31G*). Calculated geometric parameters are given together with experimental values in the respective tables. Furthermore, we calculated the vibrational frequencies with the HF/3-21G method. The Cartesian force constants were multiplied with a scale factor of 0.85 except for torsional vibrations, which were not scaled. Vibrational amplitudes were derived from this force field with the program ASYM40.²² Geometric parameters for the syn conformer of PAN (without dihedral angles), derived with the B3LYP method, have been reported in the literature.²³ When our studies were completed, we learned about recent quantum chemical calculations (MP2 and B3LYP with 6-31G* basis sets) for PAN.²⁴ In these structure optimizations, however, the O—C and C—C single bond lengths were erroneously set to be equal. Therefore, these results do not correspond to a correct structure optimization and the MP2 values do not agree with ours, neither regarding structural parameters nor energy differences.

Discussion

In the GED experiment for PAN and FPAN and in the microwave spectra for FPAN only, the syn conformer (C=O bond syn to O—O bond) was observed, in agreement with our theoretical calculations. These calculations reproduce all geometric parameters satisfactorily except for the O—N bond length. The HF/3-21G values are slightly too short, and the MP2/6-31G* values are too long by 0.05–0.06 Å. Only the DFT method reproduces these distances correctly.

Table 8 compares skeletal geometric parameters of some peroxides with electron-withdrawing substituents. The atom bonded to the peroxide group is either an sp³-hybridized carbon

atom (CF₃) or an sp²-hybridized carbon (RC(O)) or nitrogen atom (NO₂). The O—O bond lengths in these compounds vary between 1.41 and 1.42 Å and are considerably shorter than those in peroxides with electropositive substituents (1.464 Å in HOOH,²⁹ 1.457(12) Å in MeOOME³⁰). The most interesting geometric parameter in the peroxy nitrates is the O—N bond length, which correlates with their low thermal stability. These bonds (1.49–1.53 Å) are extremely long compared to those of covalent nitrates with electropositive substituents (1.383(5) Å in Me₃SiONO₂,³¹ 1.406(5) Å in HONO₂,³² and 1.402(5) Å in MeONO₂³³). In some peroxides this bond is even longer than that in FONO₂ (1.507(4) Å).³⁴ The O—N bond in PAN (1.492(7) Å) is remarkably shorter than that in FPAN (1.526(10) Å). This is surprising because the experimental O—N bond energies (28(1) kcal mol⁻¹) are equal within their experimental uncertainties^{3,9} and four bonds lie between the H or F and the O—N bond. On the other hand, the experimental trend is reproduced very well by the computational methods, which predict this bond to be 0.02–0.04 Å shorter in PAN than in FPAN (see Tables 1 and 3). The dihedral angles around the O—O bond are smaller than 90° in peroxides with two sp²-hybridized substituents (RC(O) or NO₂). If both substituents are sp³-hybridized, the dihedral angle is about 120° (123.3(40)° in CF₃OOCF₃²⁵ and 119(4)° in MeOOME³⁰). This angle is intermediate in CF₃OONO₂ (105.1(16)°²⁸), which contains one sp³- and one sp²-hybridized substituent.

Acknowledgment. Financial support by the Deutsche Forschungsgemeinschaft and the Fonds der Chemischen Industrie is gratefully acknowledged.

IC001077R

- (21) Frisch, M. J.; Trucks, G. W.; Schlegel, H. B.; Gill, P. M. W.; Johnson, B. G.; Robb, M. A.; Cheeseman, J. R.; Keith, T.; Petersson, G. A.; Montgomery, J. A.; Raghavachari, K.; Al-Laham, M. A.; Zakrzewski, V. G.; Ortiz, J. V.; Foresman, J. B.; Cioslowski, J.; Stefanov, B. B.; Nanayakkara, A.; Challacombe, M.; Peng, C. Y.; Ayala, P. Y.; Chen, W.; Wong, M. W.; Andres, J. L.; Replogle, E. S.; Gomperts, R.; Martin, R. L.; Fox, D. J.; Binkley, J. S.; Defrees, D. J.; Baker, J.; Stewart, J. P.; Head-Gordon, M.; Gonzalez, C.; Pople, J. A. *Gaussian 94*, revision B.1; Gaussian, Inc.: Pittsburgh, PA, 1995.
- (22) Hedberg, L.; Mills, I. M. *J. Mol. Spectrosc.* **1993**, *160*, 117.
- (23) Jursic, B. S. *J. Mol. Struct.: THEOCHEM* **1996**, *370*, 65.
- (24) Mhin, B. J.; Chang, W. Y.; Lee, J. Y.; Kim, K. S. *J. Phys. Chem A* **2000**, *104*, 2613.

- (25) Marsden, C. J.; Bartell, L. S.; Diodati, F. P. *J. Mol. Struct.* **1977**, *39*, 253.
- (26) Mack, H.-G.; Della Védova, C. O.; Oberhammer, H. *Angew. Chem.* **1991**, *103*, 1166; *Angew. Chem., Int. Ed. Engl.* **1991**, *30*, 1145.
- (27) Scheffler, D.; Schaper, I.; Willner, H.; Mack, H.-G.; Oberhammer, H. *Inorg. Chem.* **1997**, *36*, 339.
- (28) Kopitzky, R.; Willner, H.; Mack, H.-G.; Pfeiffer, A.; Oberhammer, H. *Inorg. Chem.* **1998**, *37*, 6208.
- (29) Koput, J. *J. Mol. Spectrosc.* **1986**, *115*, 438.
- (30) Haas, B.; Oberhammer, H. *J. Am. Chem. Soc.* **1984**, *106*, 6146.
- (31) Hertel, T.; Jakob, J.; Minkwitz, R.; Oberhammer, H. *Inorg. Chem.* **1998**, *37*, 5092.
- (32) Cox, A. P.; Riveros, J. M. *J. Chem. Phys.* **1965**, *42*, 3105.
- (33) Cox, A. P.; Waring, S. *Trans. Faraday Soc.* **1971**, *67*, 3441.
- (34) Casper, B.; Dixon, D. A.; Mack, H.-G.; Ulic, S. E.; Willner, H.; Oberhammer, H. *J. Am. Chem. Soc.*, **1994**, *116*, 8317.